

The elemental composition of virus particles: implications for marine biogeochemical cycles

Luis F. Jover¹, T. Chad Effler², Alison Buchan², Steven W. Wilhelm² and Joshua S. Weitz^{1,3}

Abstract | In marine environments, virus-mediated lysis of host cells leads to the release of cellular carbon and nutrients and is hypothesized to be a major driver of carbon recycling on a global scale. However, efforts to characterize the effects of viruses on nutrient cycles have overlooked the geochemical potential of the virus particles themselves, particularly with respect to their phosphorus content. In this Analysis article, we use a biophysical scaling model of intact virus particles that has been validated using sequence and structural information to quantify differences in the elemental stoichiometry of marine viruses compared with their microbial hosts. By extrapolating particle-scale estimates to the ecosystem scale, we propose that, under certain circumstances, marine virus populations could make an important contribution to the reservoir and cycling of oceanic phosphorus.

Dissolved organic matter (DOM). Operationally defined as marine organic matter that passes through a filter with pores of 0.22 µm to 0.45 µm in diameter. DOM can be further classified on the basis of biological availability.

Particulate organic matter (POM). Operationally defined as the material in a marine environment that is retained by a filter with pores of 0.22 µm to 0.45 µm in diameter.

Viruses in marine environments have received considerable attention over the past 2 decades. The lysis of host cells by marine viruses releases dissolved organic matter (DOM) and particulate organic matter (POM) back into the environment, where it can be assimilated by microorganisms or exported from surface waters to the deep ocean. This process of virus-mediated recycling of organic matter — which is known as the ‘viral shunt’ — is at the centre of many discussions concerning marine geochemical cycles^{1–5}. Indeed, viruses are major drivers of the mortality of both phytoplankton and heterotrophic bacteria⁵. The lysis of bacterial cells by viruses (that is, by bacteriophages) and the lysis of eukaryotic host cells by viruses releases previously cell-bound organic material that might facilitate the growth of the remaining community members^{6–8} (FIG. 1).

Prior efforts to characterize the viral shunt have mainly focused on the amount of organic material that is released by the lysis of microbial host cells, using carbon as a ‘proxy currency’. Here we focus on the often overlooked fact that the organic matter that is released following cell lysis includes virus particles. Although previous work did consider the mass of virus particles, the focus was mainly on the carbon content; for example, Wilhelm and Suttle¹ estimated that marine viruses contained 0.2 fg carbon per virus particle, and this estimate has been carried forward in other studies^{5,9}. Steward *et al.*¹⁰ more recently estimated that marine viruses

contained 0.055 fg carbon per virus particle by assuming that viruses are composed of equal parts DNA and protein¹¹ and leveraging the distributions of lengths of marine virus genomes. Viruses differ in capsid size and structure as well as in genome sequence, and these markedly different estimates of the carbon content of virus particles (0.055–0.2 fg carbon per particle) might reflect the inherent variability across a range of virus types within a community. However, irrespective of this variation, marine virus particles are substantially smaller — in terms of overall mass — than their bacterial hosts; for example, for cyanobacteria, the amount of carbon per cell has been estimated to be between 50 fg per cell and 250 fg per cell¹², and for heterotrophic bacteria, the estimated range is 20–100 fg per cell¹³. In both cases, a bacterial cell is predicted to contain at least two orders of magnitude more carbon than a virus particle. It is therefore not surprising that the relative contribution of virus particles to the total magnitude of the viral shunt and dissolved organic carbon (DOC) reservoirs has not been highlighted previously. However, ignoring the content and contribution of virus particles could become more problematic when we turn our attention to nitrogen and phosphorus.

The baseline for studies of the elemental stoichiometry of marine microorganisms was established more than 60 years ago by Alfred Redfield, who estimated that marine plankton (and organic marine detritus) have a

¹School of Physics, Georgia Institute of Technology, Atlanta, Georgia 30332, USA.

²Department of Microbiology, University of Tennessee, Knoxville, Tennessee 37996, USA.

³School of Biology, Georgia Institute of Technology, Atlanta, Georgia 30332, USA. Correspondence to J.S.W. e-mail: jsweitz@gatech.edu doi:10.1038/nrmicro3289

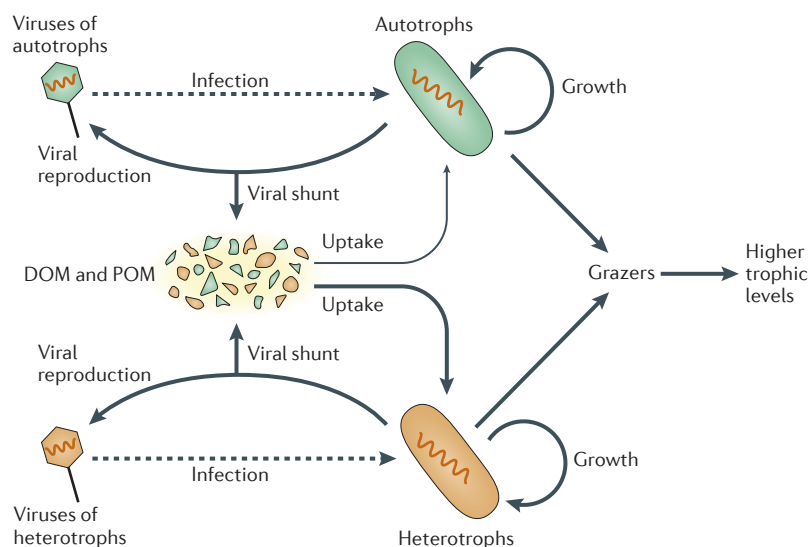


Figure 1 | Schematic of the viral shunt. Virus-mediated lysis of microbial cells releases dissolved organic matter (DOM) and particulate organic matter (POM) back into the microbial loop, rather than these cells being targeted by grazers (for example, nanozooplankton and microzooplankton), which can then be consumed by larger organisms in the aquatic food web. Figure adapted, with permission, from REF. 22, Faculty of 1000 Ltd.

carbon/nitrogen/phosphorus (C/N/P) ratio of 106/16/1 (REF. 14). The Redfield ratio remains the foundation for studies of the elemental composition of marine microorganisms and organic matter, particularly in the deep oceans^{4,15}. Indeed, the observed elemental ratios can vary greatly with the component of marine organic biomass that is under consideration; for example, estimates of C/N/P for marine heterotrophic bacteria are reported to be around 69/16/1 (REF. 5), and measurements for individual cyanobacterial isolates include 46/10/1 (for *Prochlorococcus* sp. MED4 under phosphorus-replete conditions) and 301/49/1 (for *Synechococcus* sp. WH8013 under phosphorus-limited conditions)¹². Thus, the elemental stoichiometry of bacterial cells varies with taxa and growth conditions and often differs substantially from the Redfield ratio (reviewed in REF. 16). Virus particles do not require the same relative investment in carbon for structural integrity and other functions as their hosts, as they are predominantly composed of proteins and nucleic acids (although many eukaryotic viruses¹⁷ and a few bacteriophages^{18,19} contain lipids). Proteins are enriched in nitrogen and nucleic acids are enriched in both nitrogen and phosphorus compared with the typical contents of a microbial cell. Hence, it should be expected that **virus particles are enriched in both nitrogen and phosphorus relative to carbon when compared with microorganisms**. We are aware of **only one previous example in which the entire carbon, nitrogen and phosphorus content of a virus was enumerated: the elemental stoichiometry of *Paramecium bursaria Chlorella virus 1* (PBCV1)**, which is a relatively large virus that infects the freshwater alga *Chlorella* NC64A, was estimated to be 17/5/1 (REF. 20). Calculating the elemental stoichiometry of PBCV1 was intended to test the consequences of stoichiometric differences between

the virus and its algal host. However, neither the elemental content of virus particles nor the fraction of dissolved organic nitrogen (DON) and dissolved organic phosphorus (DOP) that is partitioned in viral populations has been systematically studied so far.

In this Analysis article, we use an *ab initio* approach to **predict the elemental content of virus particles**, with a focus on **bacteriophages**. This unified biophysical and biochemical model is generalizable and enables the **prediction of the elemental content and ratios** that are present in **bacteriophage particles** of varying sizes. We leverage this model to estimate how much of the carbon, nitrogen and phosphorus that is released following the phage-induced lysis of an individual bacterial host cell is bound in cellular debris and how much is integrated in progeny bacteriophage particles. Then, we scale up these particle-level estimates to estimate the **amount** of the **DOC, DON and DOP that is partitioned in virus populations in marine surface waters** in order to begin to **quantify the relevance of virus particles** to marine biogeochemical pools and fluxes.

The elemental composition of virus particles

Virus particles are commonly composed of a head and, in some cases, a tail. The two major components of the head are the capsid, which comprises a protein shell that is usually one single protein layer thick²¹, and the genetic material that is packed inside it, which is either DNA or RNA. In this section, we use a geometric model of the viral head to estimate the number of macromolecules that comprises each of its components, that is, the number of proteins in the capsid and the number of nucleotides in the genetic material. We focus on double-stranded, icosahedral and spherical DNA bacteriophages that do not contain lipids, but the model could be extended to consider different viral shapes or types.

The basis for our model is an approximation of the virus head as a spherical shell with a fraction of its internal volume filled by DNA (FIG. 2a). The spherical shell can be described in terms of its external radius, which denotes the distance from the centre of the capsid to its outer boundary. The expected number of base pairs inside the capsid, is:

$$n_{bp} = \text{fill} \frac{v_{ic}}{v_{bp}} = \text{fill} \frac{4\pi}{3v_{bp}} (r_c - h)^3 \quad (1)$$

where v_{ic} is the volume inside the capsid, fill is the volume-filling fraction of the DNA inside the capsid, h is the thickness of the capsid and v_{bp} is the volume of a base pair.

To estimate the quantity of proteins in the capsid, each with average volume, we assume that the capsid is a spherical shell that has a uniform thickness taking up a volume. The expected number of capsid proteins is:

$$n_{pr} = \frac{v_c}{v_{pr}} = \frac{4\pi}{3v_{pr}} (r_c^3 - (r_c - h)^3) \quad (2)$$

An expression for the number of proteins as a function of the number of base pairs can be obtained using equation 1 to obtain r_c as a function of n_{bp} and substituting this result into equation 2. It can be seen from

Heterotrophic bacteria
Bacteria that use organic carbon compounds to satisfy nutritional requirements.

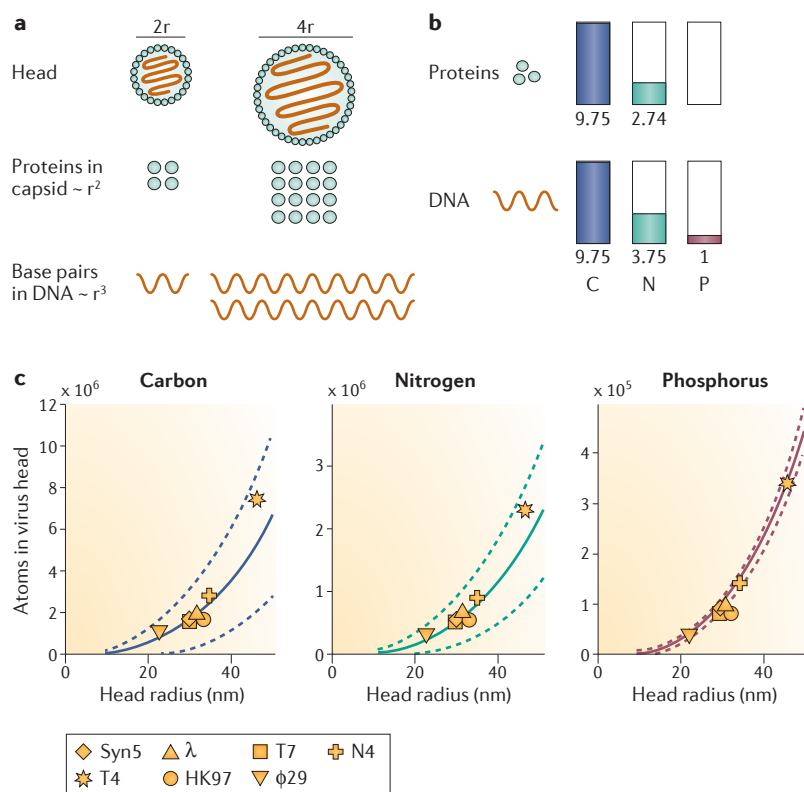


Figure 2 | Model of the elemental stoichiometry of virus particles. **a** | The viral head is approximated as a spherical shell of proteins with an internal core of nucleic acids. The number of proteins scales with the radius of the capsid squared (r^2) and the number of base pairs scales with the radius of the capsid cubed (r^3). **b** | The relative carbon, nitrogen and phosphorus content within proteins and nucleic acids. **c** | The carbon, nitrogen and phosphorus content of the viral head as a function of its external radius (solid lines). The data correspond to experimentally obtained carbon, nitrogen and phosphorus contents for different viral heads. The protein compositions of the capsids were obtained from the following references: T4 (REF. 84), N4 (REF. 79), Syn5 (REF. 80), λ and T7 (REF. 21), HK97 (REF. 81), ϕ 29 (REF. 83). The model predictions are: $C_{\text{head}} = 41(r_c - 2.5)^3 + 130(7.5r_c^2 - 18.75r_c + 15.63)$, $N_{\text{head}} = 16(r_c - 2.5)^3 + 36(7.5r_c^2 - 18.75r_c + 15.63)$ and $P_{\text{head}} = 4.2(r_c - 2.5)^3$, where r_c is in units of nm. The basis for model error estimates (dashed lines) is detailed in Supplementary information S1 (box). The estimate of the scaling between genome length and virus capsid radius (Supplementary information S1 (box)) is key.

equation 1 and equation 2 that the number of proteins in the capsid scales, to leading order, with the square of the viral radius — that is, the number of proteins in the capsid is proportional to the capsid surface area — and that the number of nucleotides scales, to leading order, with the cube of the viral radius — that is, the number of nucleotides is proportional to the internal volume of the capsid (FIG. 2a). This size-dependent scaling of macromolecular content is crucial to characterize the size-dependent scaling of elemental content within virus particles. To complete our biophysical scaling model of the elemental stoichiometry of virus heads, we incorporated the average elemental composition of proteins and nucleotides (proteins contain carbon and nitrogen but not phosphorus, whereas DNA (and RNA) contains carbon, nitrogen and phosphorus (FIG. 2b)). A complete list of biophysical and biochemical constants can be found in [Supplementary information S1](#) (box); the raw data

supporting the calculations in the box are available in [Supplementary information S2](#) (table), [Supplementary information S3](#) (table) and [Supplementary information S4](#) (table).

Our estimates of the elemental content in virus tails follow a similar logic. The virus tail, when present, is comprised of tyre-shaped protein subunits. Hence, we approximate the tail structure as a hollow cylinder with outside radius r_t , fixed thickness h_t , and length l_t . The number of proteins in the tail is then estimated by dividing the tail volume by the volume of a protein. The abundance of carbon and nitrogen atoms in the tail is the product of the number of proteins and the average carbon and nitrogen content of proteins; unlike virus heads, virus tails should not contribute to the total phosphorus content of virus particles (for details of the calculation, see [Supplementary information S1](#) (box)).

Elemental stoichiometry depends on virus size

The theoretical model predictions for the elemental composition of viral heads were validated using data for seven bacteriophages that infect either heterotrophic bacteria or cyanobacteria (TABLE 1). These bacteriophages were chosen as complete genome sequences, structural characterization (that is, the full complement of viral head proteins and their stoichiometry) and the amino acid sequences for all of the head protein components were publicly available. The elemental composition of each bacteriophage particle was calculated from the genome sequence (carbon, nitrogen and phosphorus) and the protein stoichiometry and amino acid content of each protein in the capsid (carbon and nitrogen only). The predictions of elemental abundance that were obtained using the biophysical scaling model strongly agreed with those that were directly measured for the seven reference phage heads (FIG. 2c; TABLE 1; [Supplementary information S1](#) (box)), which suggests that the model can be used to predict the size-dependence of the elemental stoichiometry of intact virus particles.

To evaluate contributions from viral tails, the carbon, nitrogen and phosphorus content was calculated for three viruses (T4, N4 and Syn5) for which there is detailed structural information available about both the head and tail ([Supplementary information S1](#) (box)). Tail inclusion modestly increased the total carbon and nitrogen content but not the phosphorus content ([Supplementary information S1](#) (box)). Thus, considering the head size (or genome length) alone will lead to underestimates of ~2–14% for total carbon and nitrogen content in viral particles, and the degree of underestimation depends on the size of the tail relative to the head. The ratio of tail to head size can be quantified when quantitative transmission electron microscopy (qTEM) data are available ([Supplementary information S1](#) (box)).

As is apparent, the elemental content of virus particles will scale with size. To account for this effect in the case of virus heads, our biophysical model assumes that the capsid surface layer is composed of proteins, and hence the total number of proteins scales, approximately, with the genome length raised to the power of two-thirds. Large viruses will have relatively higher proportions of

Cyanobacteria

Ubiquitous marine bacteria that fix inorganic carbon compounds into organic carbon compounds.

Quantitative transmission electron microscopy (qTEM)

Method to quantitatively estimate viral morphological characteristics (such as morphotype, capsid diameter and tail length) using transmission electron microscopy.

Table 1 | Elemental composition, genome lengths and radii of selected viral heads

Virus	Carbon (atoms)	Nitrogen (atoms)	Phosphorus (atoms)	C/N/P*	Genome length (bp)*	Radius (nm)	Refs
Enterobacteria phage T4	7,339,851	2,309,461	337,806	22.3/6.6/1	168,903	46.3 [§]	78,84
<i>Escherichia</i> spp. phage N4	2,765,271	891,989	140,306	17.9/5.9/1	70,153	34.8	79
<i>Synechococcus</i> phage Syn5	1,664,612	563,058	92,428	17.3/5.9/1	46,214	30	80
Enterobacteria phage λ	1,897,088	621,823	97,004	19.2/6.3/1	48,502	31.5	21,78
Enterobacteria phage HK97	1,640,059	536,465	79,464	20.6/6.8/1	39,732	33	81
Enterobacteria phage T7	1,550,638	517,474	79,874	18.1/6.1/1	39,937	30	21,82
<i>Bacillus</i> spp. phage Φ29	1,058,584	326,209	38,564	23.3/7.3/1	19,282	22.8 [§]	83

*Composition based on sequence information and experimentally validated stoichiometry of structural proteins. †The GenBank accession numbers of the DNA sequences are: [NC_000866.4](#) (T4), [NC_008720.1](#) (N4), [NC_009531.1](#) (Syn5), [NC_001416.1](#) (λ), [NC_002167.1](#) (HK97), [NC_001604.1](#) (T7), [NC_011048](#) (φ29). §The reported radius is equivalent to that of the sphere with the same volume as an ellipsoid with the dimensions of the corresponding phage prolate head.

phosphorus, as the number of phosphorus atoms scales with the number of nucleotides. As large viruses (viruses that have capsid diameters that are greater than 100 nm) are considered, the elemental ratios of the virus particles would approach the elemental ratios of their nucleic acids asymptotically. Considering only C/N ratios initially, viruses of any size are predicted to have ratios that are similar to that of their DNA (FIG. 3). By contrast, when considering N/P ratios, virus size matters — the N/P ratios of large viruses are predicted to be similar to that of their DNA, whereas the N/P ratios of small viruses are predicted to approach the Redfield ratio (FIG. 3).

Stoichiometric mismatch between virus and host

Virus-induced host cell lysis releases virus particles and cellular debris into the environment; cellular debris is released in the form of DOM and POM. It has been suggested that the elemental stoichiometry of the lysed

contents may be different from that of the original host cell^{5,22}. The difference in the elemental contents of viruses and their hosts (an example of ‘stoichiometric mismatch’ (REF. 16)) has the potential to drive the differential release of nutrients following cell lysis. In this section, we use our scaling model for viral C/N/P to consider the role of virus-mediated lysis in transforming the elemental stoichiometry of released organic matter into two components that have potentially different stoichiometries and proportions: cellular debris and virus particles.

The amount of material that is released following cell lysis can be predicted on the basis of the following principle of conservation of elements:

$$X_{\text{lysis}} = X_{\text{host}} - \beta X_{\text{virus}} + X_{\text{acquired}} \quad (3)$$

where X is the element of interest and β is the burst size (that is, the number of virus particles that is released from each lysed host cell). The subscripts denote the elemental content that is released as cellular debris (X_{lysis}), the content that is released in each virus particle (X_{virus}), the content that is found in the original host (X_{host}) and the content that is acquired (by uptake or fixation) after infection but before lysis (X_{acquired}). We expect that $X_{\text{acquired}} > 0$, as it is known that both resource uptake and fixation occur during viral infection and that viruses can repurpose and modify the uptake rates of nutrients; for example, phosphorus is a common limiting nutrient for marine cyanobacteria *Prochlorococcus* spp. and *Synechococcus* spp. (as can be assessed via the diagnostic product of the *pstS* gene (REF. 23)). Some cyanophage genomes that have been isolated from phosphorus-depleted ocean waters contain the *pstS* gene (REFS 24, 25), and laboratory experiments have shown that cyanophages can upregulate *pstS* expression to increase the acquisition of phosphorus during infection²⁶. Thus, cyanophage manipulation of the host phosphorus status is crucial to the elemental stoichiometry of the virus-infected cyanobacterial host cell. However, specific predictions for a host–virus system that result from equation 3 would require measurements of X_{acquired} and such data are not broadly available. Below, we consider a series of limit cases in order to gauge the sensitivity of our predictions to variations in post-infection uptake.

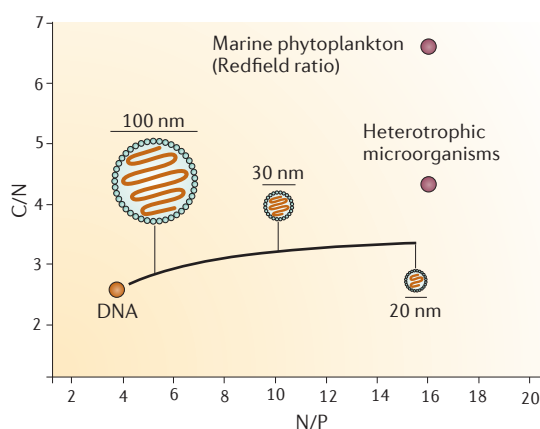


Figure 3 | Theoretical prediction of elemental stoichiometry for viruses. We compare the predicted C/N and N/P ratios for viruses (solid black line) with the ratios that are expected for DNA, marine phytoplankton (as per the Redfield ratio) and heterotrophic microorganisms. The theoretical curve (solid black line) denotes the predicted stoichiometry for viruses that have capsid diameters in the range of 20 nm to 300 nm. The stoichiometry of three representative viruses that have capsid diameters of 20 nm, 30 nm and 100 nm is shown.

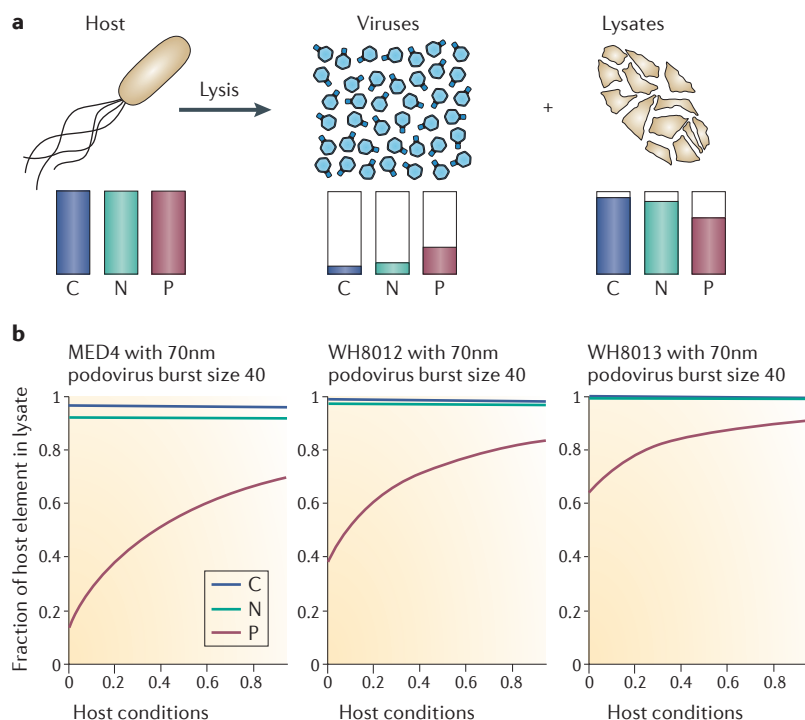


Figure 4 | Virus-induced transformation of elemental content in cellular debris following lysis. **a** | After lysis, the contents of a host are released as virus particles and other cellular debris (that is, the lysate). The relative carbon, nitrogen and phosphorus levels in the virus particles and the lysate are shown in bars; the bar height is normalized in each case by the total amount of the element in the host. Bar heights are based on the hypothetical infection of *Prochlorococcus* sp. MED4 host under phosphorus-replete conditions by a podovirus with 70 nm diameter head. Note that, in fact, the total carbon, nitrogen and phosphorus content differs between the host and the virus (FIG. 3). **b** | Predictions of the model of elemental transformation as applied to a viral infection of three marine cyanobacteria. The fraction of the host element in the lysate in each panel is normalized by the elemental content of the respective host. The x axis denotes culture conditions from phosphorus-limited (0) to phosphorus-replete (1) (REF. 12).

In the first limit case, we assume that no extracellular elements are obtained during the production of virus particles, that is, virus particles are assembled solely from organic materials that are already present in the host at the time of infection (that is, $X_{\text{acquired}} \sim 0$). This condition is likely to be relevant for some marine viruses; for example, studies of marine bacteriophage genome synthesis using radioactively labelled phosphorus found that “the majority of nucleotides used during phage DNA synthesis were derived from degraded nucleic acids (that is, DNA and RNA) of the host cell” (REF. 27). Under this scenario, how much carbon, nitrogen and phosphorus would be released as cellular debris?

To answer this, we considered a hypothetical scenario in which a podovirus with a capsid diameter of 70 nm and burst size of 40 infected distinct cyanobacterial strains (FIG. 4a). We focus on three specific host systems: the cyanobacteria *Prochlorococcus* sp. MED4, *Synechococcus* sp. WH8012 and *Synechococcus* sp. WH8103, for which the total dry masses of carbon, nitrogen and phosphorus have been measured in axenic cultures using both phosphorus-replete and phosphorus-limited culture conditions¹². We then used

equation 3 (where $X_{\text{acquired}} = 0$) to estimate the abundance of carbon, nitrogen and phosphorus contained within virus particles relative to the total carbon, nitrogen and phosphorus in the lysate (FIG. 4b).

For all three virus–host pairs, the predicted relative abundance of carbon and nitrogen in the lysate is close to 1, which indicates that most host-derived organic carbon and nitrogen was released as cellular debris rather than bound in virus particles. By contrast, phosphorus was predicted to be mostly bound within virus particles. For phosphorus-limited *Prochlorococcus* sp. MED4, the model predicts that 87% of the original phosphorus content of the cells would be converted into virus particles and only 13% would be released in the non-viral component. Although under phosphorus-replete conditions *Prochlorococcus* sp. MED4 (FIG. 3a) had a C/N/P ratio of ~120.5/21.2/1, the current model conditions predict that virus particles would have a C/N/P ratio of ~17.2/5.9/1 and the remaining cellular debris would have a C/N/P ratio of ~171.9/28.8/1. Hence, in the absence of phosphorus uptake by the infected host, the cellular materials that are released as debris (and are not bound in viruses) will be depleted in phosphorus relative to carbon and nitrogen; how much so will depend on the elemental content of the host (and the elemental availability), the size of the virus and the burst size. Indeed, when virus particles are predominantly synthesized from host elements that are available before infection, burst sizes are likely to decrease in nutrient-poor hosts; for example, smaller virus burst sizes were observed when the algal virus PBCV1 infected ‘poor-quality’ algal hosts (that is, hosts that had a high C/P ratio)²⁰. A similar phenomenon of reduced lysis (and, consequently, an increased incidence of lysogeny) has been observed during infections of phosphorus-limited *Synechococcus* sp. WH7803 hosts²⁸.

To contrast this scenario, we considered a second limit case in which virus particles are produced from elemental pools that are acquired post-infection (whereby $\beta X_{\text{virus}} = X_{\text{acquired}}$). In this scenario, there would be no change in the elemental stoichiometry of lysed materials that were not bound within virus particles. The reality is probably somewhere between these two limit cases; for example, formative studies of DNA synthesis in T-even phage infecting *Escherichia coli* suggested that new assimilation of phosphorus during infection is common, although host nucleic acids are also used for virus synthesis^{29,30}. In cyanobacteria, the assimilation of inorganic matter that is associated with viral infection augments nutrient pools that are already available in the host cell^{24–26}. The potential degree to which virus particles are formed from pre-existing or newly acquired elements can be characterized in terms of the elemental independence of the virus (ε_x), such that ε_x approaches 0 if the virus uses only host elements and acquires all of the elements that are used in production of virus particles during infection. This index can be estimated by measuring:

$$\varepsilon_x = \frac{X_{\text{acquired}}}{X_{\text{acquired}} + X_{\text{host}}} = \frac{X_{\text{lysis}} - X_{\text{host}} + \beta X_{\text{virus}}}{X_{\text{lysis}} + \beta X_{\text{virus}}} = 1 - \frac{X_{\text{host}}}{X_{\text{lysis}} + \beta X_{\text{virus}}} \quad (4)$$

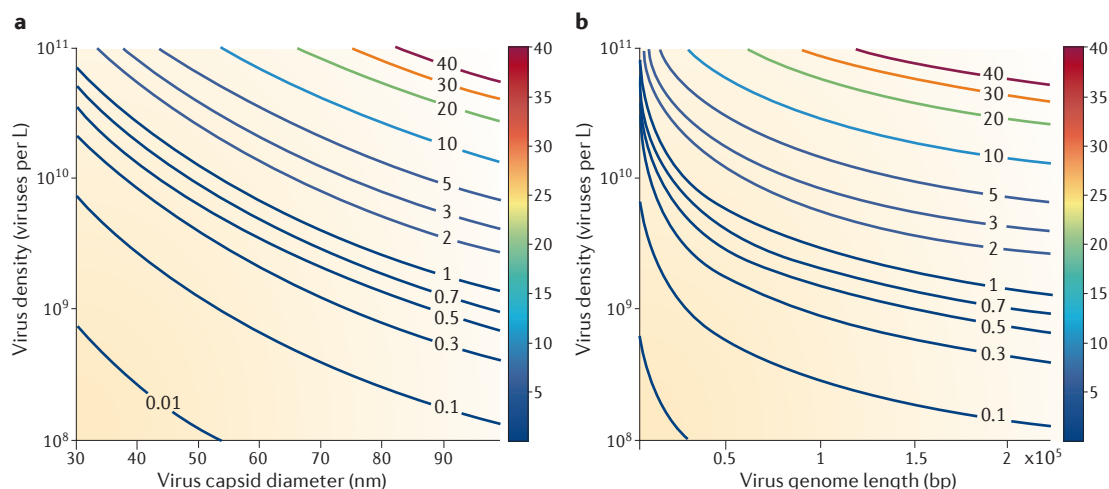


Figure 5 | Predicted DOP concentration in viral populations as a function of viral density and virus size. **a** | Virus size is quantified in terms of mean capsid diameter, which varies from 30 nm to 100 nm. **b** | Virus size is quantified in terms of genome length, which ranges from 4.1 kb to 220 kb. In both cases, viral density varies from 10^8 virus particles per litre to 10^{11} virus particles per litre on a logarithmically spaced axis. The contour lines denote combinations of viral density and capsid diameter, which correspond to the same predicted concentration of dissolved organic phosphorus (DOP) that is partitioned in viruses. The colour bar indicates the predicted DOP in units of nmol per litre.

If the \mathcal{E}_x of a virus approaches 1, then the stoichiometry of released cellular debris should approach that of the original host cell stoichiometry.

These two limit cases show that the extent to which viruses change the stoichiometry of cellular debris depends on differences between their stoichiometry and the stoichiometry of their host as well as their elemental independence. Although previous experimental studies showed that cellular debris that is released following lysis stimulates the growth of non-targeted cells^{6–8} (probably owing to the increased bioavailability of carbon (REF. 31), nitrogen (REF. 32) and iron (REF. 33)), our model predicts that the lysate tends to be depleted in nutrients relative to the host (the tendency can be characterized in terms of the parameter \mathcal{E}_x). This cellular debris may be a source of refractory matter that is relatively low in phosphorus and is not repurposed for viral production. These observations lay the groundwork for future hypothesis testing in ecologically important model systems (for example, in abundant viruses that infect pelagibacteria, cyanobacteria and roseobacteria³⁴) to determine how viruses transform cellular material into recalcitrant organic matter⁴. Such data would be invaluable for constraining the range of predictions of our model regarding the relative elemental content of cellular debris and virus particles that are released following lysis.

Marine virus particles and elemental reservoirs

The total abundance of elements in marine viruses is a product of the abundance of viruses and their per-particle elemental content, both of which can vary across space and time. Marine virus densities range from 10^8 virus particles per litre in oligotrophic systems to more than 10^{11} virus particles per litre in highly productive environments^{35–37}. Viruses (in general) and marine viruses (in particular) can vary substantially in genome

length and particle size and, consequently, in elemental content (FIG. 2; Supplementary information S1 (box)). However, to extrapolate from particle-scale results to the population scale, variation in the sizes of marine virus particles must be taken into account.

We first examined the expected phosphorus content of marine virus populations. In FIG. 5a, we show the predicted DOP concentration (in nmol per litre) that is bound in virus populations if virus densities are in the range of 10^8 to 10^{11} virus particles per litre and virus capsid sizes are 30–100 nm. Likewise, in FIG. 5b, we show the predicted DOP concentration (in nmol per litre) that is bound in virus populations, using the same range of virus densities but considering ranges of virus genomes from 4.1 kb to 220 kb (as derived on the basis of our scaling model). The total DOP content of a virus population that comprises identically sized virus particles ranges from less than 0.1 nM (in the limit of low densities and small particles) to greater than 40 nM (in the limit of high densities and large particles). However, we can narrow this range on the basis of the global qTEM survey of marine viruses by Brum *et al.*³⁸. This qTEM study found that most virus capsids have diameters of 50–70 nm and that individual capsid diameters range from 20 nm to 200 nm (REF. 38). Restricting our extrapolation to populations that have average capsid diameters in the 50 nm to 70 nm range, we predict a range of 0.0025 fg to 0.0074 fg phosphorus per particle. Hence, as marine virus densities range from 10^8 virus particles per litre to 10^{11} virus particles per litre, we predict that marine virus populations contain 0.0079–24 nM DOP. These predictions rely on our model of virus heads only, as any underestimates of elemental content owing to contributions from virus tails would affect carbon and nitrogen predictions but not phosphorus predictions.

By means of comparison, DOP estimates across multiple oceanic realms, including the Alaskan Gyre, North

Oligotrophic

A term used to describe an aquatic environment that has low levels of nutrients and photosynthetic production (for example, the open ocean).

Sea, North Pacific Ocean, North Pacific Gyre, Subtropical North Atlantic, Southeast Pacific and Southern Ocean, range from 30 nM to 300 nM (REFS 39–48). DOP can constitute more than 80% of the total dissolved phosphorus pool in marine surface samples⁴³. The structural characterization (including solid-state ³¹P-NMR (REFS 40, 49)) of compounds in the DOP pool does not rule out nucleic acids as important constituents. Hence, it is likely that virus particles are included in these estimates, even if their contribution to the total DOP was not specifically identified. It is evident that the upper ranges of DOP that is bound in viral populations approach the lower ranges of the total DOP pool size that was measured in marine surface waters. Considering the extremes of these ranges, we find that virus populations may potentially account for anything from <0.01% of the total DOP pool (when dividing the lower value of 0.0079 nM that is bound in viruses with the upper value of 300 nM in the total pool) to >50% of the total DOP pool (when dividing the upper value of 24 nM that is bound in viruses with the lower value of 30 nM in the total pool). However, dividing the limits of two biological ranges does not fully take into account the potential correlations between DOP and virus abundance. Hence, we use three case studies — the Sargasso Sea, Station ALOHA in the North Pacific Ocean Subtropical Gyre and a coastal site in the Southern Pacific Ocean — to illustrate circumstances in which virus populations are likely to have distinct degrees of importance with respect to the proportion of DOP that is partitioned in marine surface waters.

The Bermuda Atlantic Time-series Study (BATS) has collected oceanographic data in the Sargasso Sea, which is a well-studied open-ocean environment in the Atlantic Ocean, for 25 years. Assuming that DOP makes up 80% of the total dissolved phosphorus at BATS (REF. 43), then 95% of DOP measurements from 2000–2009 range from 25 nM to 109 nM, with an average of 58 ± 22 nM (REF. 50). Given decadal measurements (in 2000 and 2009) of seasonally varying virus abundances at BATS⁵¹, we predict that the fraction of Sargasso Sea DOP that is partitioned in viruses is in the range of 0.10% to 8.0% (TABLE 2). Similarly, the Hawaii Ocean Time series (HOT) programme includes more than 25 years of oceanographic data, which has been collected within the North Pacific Subtropical Gyre, including a deep-water site (Station ALOHA) near to the island of Oahu, Hawaii. The data that were collected at Station ALOHA include measurements of DOP, such that 95% of the DOP measurements that were made between 1988 and 2012 range from 150 nM to 320 nM, with an average of 224 ± 46 nM (REF. 52). When these DOP ranges (and in one case, concurrent measurements of DOP) are compared with two marine virus surveys that were conducted at this site^{53,54}, we predict that the fractional DOP that is bound in virus populations at HOT ranges between 0.15% and 1.5%. Hence, at both the BATS and HOT sites, we predict that viruses do not generally make up a significant fraction of the DOP pool, although they can potentially exceed 5% of the total DOP pool at BATS (TABLE 2).

Table 2 | **Viral and non-viral components of DOP in marine surface waters**

Data set	Site information (for virus survey)	Virus abundance (virus particles per litre)	Estimated DOP in virus particles (nM)*	Total DOP in surface waters (nM)	Estimated % of total DOP bound in virus particles†	Refs
Marine virus surveys		10^8 – 10^{11}	<0.01–24			5,35–37
Marine DOP surveys				30–300		39–48
Atlantic Subtropical Gyre (BATS)	Late summer 2000–2009; depth: 60–100 m	6 – 12×10^9	0.48–2.9	58 ± 22 (station average)	0.61–8.0%	43,50,51
	Stratified summer 2000–2009; depth: 0–20 m	1 – 3×10^9	0.081–0.72	58 ± 22 (station average)	0.10–2.0%	43,50,51
North Pacific Subtropical Gyre (HOT), open-ocean site	September 1998; depth: 0–100 m	4.5 – 5.5×10^9	0.36–1.3	230 ± 20 (concurrent)	0.15–0.63%	52,53
	December 2002; depth: 0–100 m	8 – 11.3×10^9	0.65–2.7	224 ± 46 (station average)	0.24–1.5%	52,54
South Pacific Ocean and Southern Ocean (including open ocean and near-coastal sites)	South West New Zealand, Coastal; Sep–Oct 2008; depth: ~5 m	17 – 120×10^9	1.4–29	150–225*	0.61–19%	42,55
	Australian Southern Ocean; Jan–Feb 2007; depth: 0–40 m	6.1 – 26×10^9	0.49–6.2	150–225*	0.22–4.1%	42,58
	Drake Passage, Greenwich Meridian and Weddell Sea; Feb–Apr 2008; depth: 0–100 m	0.1 – 7.6×10^9	<0.01–1.8	150–225*	<0.01–1.2%	42,57

BATS, Bermuda Atlantic Time-series Study; DOP, dissolved organic phosphorus; HOT, Hawaii Ocean Time-series. *The range of estimated DOP in virus particles was inferred by multiplying virus abundance by the phosphorous content per particle, using 50 nm head diameter for the lower range and 70 nm head diameter for the upper range (that is, 0.0025 fg and 0.0074 fg, respectively). †The percentage range of DOP bound in virus particles was estimated by dividing (lower/upper) DOP in virus particles by total DOP (upper/lower). *Comparison site of DOP measurements was separate from virus measurements (54°0'S, 176°0'W).

By contrast, estimates of virus particles that exceed 10^{11} virus particles per litre have been reported in several productive locations (that is, during spring blooms) in the southern Pacific Ocean near New Zealand^{55,56}. Given peak virus densities of 1.2×10^{11} per litre, the DOP concentration in virus populations would range from 9.7 nM to 29 nM. By contrast, peak virus abundances for open-ocean sites in the Southern Ocean are approximately four times lower^{57,58}. Simultaneous measurements of DOP and virus abundances for both the coastal and open-ocean Southern Pacific Ocean and Southern Ocean sites are not available. As a proxy, we note that the total DOP in the upper 100 m of an open-ocean site in the Southern Ocean during the summer ranged between 150 nM and 225 nM (REF. 42), which is consistent with other Pacific Ocean estimates (for example, 100–200 nM (REF. 46)). Hence, we predict that the fraction of DOP that is partitioned in viruses during spring blooms would have exceeded 5% if the DOP concentration at coastal sites was similar to DOP concentrations elsewhere (TABLE 2).

We carried out a similar analysis for the contribution of virus particles to DOC and DON using our biophysical model. We predict that marine viruses have a carbon content that ranges from 0.02 fg to 0.05 fg and a nitrogen content that ranges from 0.0078 fg to 0.02 fg, assuming median capsid diameters in the range of 50–70 nm. Using estimated virus densities that can reach up to 10^{11} per litre, we predict that the total carbon content that is bound in marine viruses is probably no greater than 420 nM and that the total nitrogen content is probably no greater than 140 nM. In contrast to the case of DOP, we find that viruses are unlikely to constitute a substantial fraction of DOC, which has been estimated to be 34–80 μmol per litre in marine waters⁵⁹. In the case of nitrogen, concentrations of approximately 2–7 μmol per litre (mean of $4.5 \pm 0.4 \mu\text{mol}$ per litre) have been reported in global surface waters⁶⁰; thus, the viral contribution to the DON pool could range from negligible amounts to up to 7%, depending on the system.

Taken together, our scaling model predicts that the DOP (and possibly DON) content that is bound in marine viruses is potentially larger than has been recognized. Our analysis shows that virus populations are likely to constitute an important fraction (that is, >5%) of the total DOP in marine surface waters when virus density exceeds 3.5×10^{10} virus particles per litre and the total DOP concentration is approximately 100 nM (FIG. 5). Note that, although coincident measurements of virus population sizes and DOP are few in number, virus densities that approach or exceed 10^{11} virus particles per litre have been reported at multiple stations, including in an estuary (Chesapeake Bay)⁶¹, the North Sea⁶² and the Coastal Northeastern Pacific Ocean³⁵ (reviewed in REF. 37). Efforts to quantify the relative contribution of viruses to the total DOP should also consider estimates of virus turnover rates. Virus particles in marine surface waters have lifespans on the scale of hours to days^{57,58,63,64}. Hence, the DOP pool that is bound in virus particles is likely to be turned over quickly relative to other components of the DOP pool, which have been

estimated to turn over in the order of days to weeks (for example, at BATS (REF. 65)). The availability of nutrient-rich virus particles at high densities suggests that virus particles may be a target for consumption by certain marine zooplankton, particularly if ingestion does not entail an infection risk. Indeed, 20 year-old observations of nanoflagellate ingestion and digestion of viruses and virus-sized particles suggest that such digestion can and does occur⁶⁶. The importance of this target pool will depend on virus abundance and diversity, particularly in nutrient-limited regions of the ocean, and warrants renewed exploration.

Conclusions

Our analyses provide a foundation from which to evaluate the quantitative role that marine viruses have in the storage and recycling of DOC, DON and DOP. The key logical underpinning of the model is the fact that changes in the surface/volume ratio, combined with the known differential composition of proteins (which contain carbon and nitrogen but not phosphorus) and nucleotides (which contain carbon, nitrogen and phosphorus), are sufficient to make quantitative predictions regarding the elemental content of virus particles of different sizes. These particle-scale estimates can be extrapolated to ecosystem scales using marine virus survey data. Our analysis leads us to two important conclusions: first, the stoichiometric mismatch between marine viruses and their hosts provides a mechanism for the differential recycling of organic matter via the viral shunt; and second, virus particles have the potential to contribute an important component of the DOP (and, in some cases, the DON) of marine surface waters.

Although we have focused on marine bacteriophage particles, our conclusions probably apply to marine viruses generally, including viruses of archaea and eukaryotes, such as algae. Irrespective of the specific host that is involved, the elemental stoichiometry of viruses should be enriched in nitrogen and phosphorus relative to the baseline elemental stoichiometry of the host cells (as has been confirmed in the case of the algae-infecting virus PBCV1 (REF. 20)). The rationale is that the structural requirements for viruses are relatively small compared with those of their hosts (with the possible exception of 'giant' viruses, which contain carbon-rich structures, including lipids and complex carbohydrates^{67,68}). We predict that there will be a stoichiometric mismatch between viruses and their hosts, leading to the depletion of nitrogen and phosphorus in cellular debris relative to host cells. Quantitative predictions of the carbon, nitrogen and phosphorus content of virus particles, broken down by virus type, may require specific extensions of the present model; this is an issue of continued interest owing to the continual discovery of novel viruses in the ocean, some of which occur at high densities (for example, single-stranded RNA (ssRNA) viruses⁶⁹), and the discovery of virus-like particles, such as gene-transfer agents⁷⁰. We suggest that further rigorous estimates of the total phosphorus, accompanied by characterization of the chemical nature of DOP in seawater (for an example, see REF. 71), will help to elucidate the relative

Spring blooms

Annual increases in phytoplankton abundance in response to seasonal changes, such as increased temperature and higher nutrient levels.

Gene-transfer agents

Phage-like particles that encapsulate cellular DNA that can be transferred to another bacterium.

contributions of viruses to the total DOP pool. Despite the need for simplification, the benefit of building a biophysical model is that it helps to identify potential differences in drivers of elemental content between viruses.

Our analysis of the stoichiometry of released materials also suggests that elemental acquisition by infected cells is important. Marine viruses can change the elemental assimilation rates of their infected hosts; for example, a recent study of lytic viral infections of marine *Prochlorococcus* spp. showed post-infection redirection of host metabolism towards increased assimilation of limiting elements (in this case, phosphorus) that might benefit the phage²⁶. This study is consistent with the previous identification and annotation of phosphorus metabolism genes²⁴ and nitrogen metabolism genes²⁵ in viral genomes, which suggests that virus-mediated repurposing of cellular metabolism occurs during infection. Further exploration is warranted to quantify the relative rates at which viruses repurpose host elements and acquire new elements post-infection (for example, as in REFS 25, 27). We anticipate that viruses that have less elemental independence from their hosts are more likely to release cellular debris with a stoichiometry that is distinct from that of the host and are thus potentially more recalcitrant to subsequent assimilation that stimulates

secondary production. Quantifying the consequences of the stoichiometric mismatch of viruses and their hosts may provide insights into the export of carbon-rich organic matter into the deep ocean⁴, in much the same way that the stoichiometric mismatch between herbivores and plants and between decomposers and plant litter has improved our understanding of nutrient cycling and the storage and regeneration of organic matter in terrestrial systems¹⁶.

In summary, this Analysis article advances long-standing efforts to quantify the relative contribution of viruses to the pools and fluxes of DOC, DON and DOP in the global oceans. In doing so, our results further highlight the importance of using classic morphological^{39,72–74}, biophysical³⁵ and biogeochemical techniques^{1,3}, in conjunction with modern biomolecular techniques^{75–77}, to provide insights into the effects of marine viruses on oceanic biogeochemistry. The fact that most marine microorganisms can be infected by viruses, including ubiquitous hosts, such as pelagibacteria, which were once thought to harbour no viruses³⁴, suggests that quantifying changes in nutrient assimilation by infected hosts and the partitioning of nutrients that are released from lysed hosts may have important consequences on a global scale.

- Wilhelm, S. W. & Suttle, C. A. Viruses and nutrient cycles in the sea. *Bioscience* **49**, 781–788 (1999). **This report estimates the contribution of virus-mediated lysis of marine bacteria and algae to the biogeochemical cycling of carbon, in the process of defining the 'viral shunt'.**
- Brussaard, C. P. D. *et al.* Global-scale processes with a nanoscale drive: the role of marine viruses. *ISME J.* **2**, 575–578 (2008).
- Fuhrman, J. A. Marine viruses and their biogeochemical and ecological effects. *Nature* **399**, 541–548 (1999). **This paper gives a foundational perspective on the roles of viruses in ecosystems and proposes estimates for the changes in carbon fluxes between ecosystem pools in aquatic food webs owing to virus-mediated lysis.**
- Jiao, N. *et al.* Microbial production of recalcitrant dissolved organic matter: long-term carbon storage in the global ocean. *Nature Rev. Microbiol.* **8**, 593–599 (2010). **This review discusses the production of recalcitrant carbon in marine systems and includes the viral shunt as a central component of the hypothesized production process.**
- Suttle, C. A. Marine viruses — major players in the global ecosystem. *Nature Rev. Microbiol.* **5**, 801–812 (2007).
- Gobler, C. J. *et al.* Release and bioavailability of C, N, P, Se, and Fe following viral lysis of a marine Chrysophyte. *Limnol. Oceanogr.* **42**, 1492–1504 (1997).
- Middelboe, M., Jørgensen, N. O. G. & Kroer, N. Effects of viruses on nutrient turnover and growth efficiency of noninfected marine bacterioplankton. *Appl. Environ. Microbiol.* **62**, 1991–1997 (1996).
- Noble, R. T., Middelboe, M. & Fuhrman, J. A. The effects of viral enrichment on the mortality and growth of heterotrophic bacterioplankton. *Aquat. Microb. Ecol.* **18**, 1–13 (1999).
- Suttle, C. A. Viruses in the Sea. *Nature* **437**, 356–361 (2005). **This paper provides the first global-scale diagram of the carbon cycle that includes marine viruses as an important component.**
- Steward, G. F. *et al.* Microbial biomass and viral infections of heterotrophic prokaryotes in the subsurface layer of the central Arctic Ocean. *Deep-Sea Res.* **154**, 1744–1757 (2007).
- Steward, G. F., Montiel, J. L. & Azam, F. Genome size distributions indicate variability and similarities among marine viral assemblages from diverse environments. *Limnol. Oceanogr.* **45**, 1697–1706 (2000).
- Bertilsson, S. *et al.* Elemental composition of marine *Prochlorococcus* and *Synechococcus*: implications for the ecological stoichiometry of the sea. *Limnol. Oceanogr.* **48**, 1721–1731 (2003). **This paper describes how phosphorus limitation shifts the subsequent elemental composition of marine cyanobacteria grown in culture.**
- Simon, M. & Azam, F. Protein content and protein synthesis rates of planktonic marine bacteria. *Mar. Ecol. Prog. Ser.* **51**, 201–213 (1989). **This paper shows that viruses in nutrient-limited environments are predominantly synthesized from elemental pools that are already available in host cells (for example, recycled nucleotides).**
- Redfield, A. C., Ketchum, B. H., & Richards, F. A. in *The composition of seawater. Comparative and descriptive oceanography. The sea: ideas and observations on progress in the study of the seas.* (Ed. Hill, M. N.) Vol. 2, 26–77 (Interscience Publishers, 1963).
- Jiao, N. *et al.* The microbial carbon pump and the oceanic recalcitrant dissolved organic matter pool. *Nature Rev. Microbiol.* **9**, 555 (2011).
- Stern, R. W. & Elser, J. J. *Ecological Stoichiometry: The Biology of Elements from Molecules to the Biosphere.* (Princeton University Press, 2002).
- Iyer, L. M., Aravind, L. & Koonin, E. V. Common origin of four diverse families of large eukaryotic DNA viruses. *J. Virol.* **75**, 11720–11734 (2001).
- Espejo, R. T. & Canelo, E. S. Properties of bacteriophage PM2: a lipid-containing bacterial virus. *Virology* **34**, 738–747 (1968).
- Bamford, D. H. *et al.* Constituents of SH1, a novel lipid-containing virus infecting the halophilic euryarchaeon *Haloarcula hispanica*. *J. Virol.* **79**, 9097–9107 (2005).
- Clasen, J. L. & Elser, J. J. The effect of host *Chlorella* NC64A carbon: phosphorus ratio on the production of *Paramecium bursaria* *Chlorella* Virus 1. *Freshw. Biol.* **52**, 112–122 (2008). **This study shows how virus productivity during infections decreases with decreasing host quality, and tabulates the total elemental content of a single algal virus.**
- Calendar, R. & Abedon S. T. *The Bacteriophages* (Oxford University Press, 2005).
- Weitz, J. S. & Wilhelm, S. W. Ocean viruses and their effects on microbial communities and biogeochemical cycles. *F1000 Biol. Rep.* **4**, 17 (2012).
- Scanlan, D. J. *et al.* An immunological approach to detect phosphate stress in populations and single cells of photosynthetic picoplankton. *Appl. Environ. Microbiol.* **63**, 2411–2420 (1997).
- Sullivan, M. B. *et al.* Three *Prochlorococcus* cyanophage genomes: signature features and ecological interpretations. *PLoS Biology* **3**, e144 (2005).
- Sullivan, M. B. *et al.* Genomic analysis of oceanic cyanobacterial myoviruses compared with T4 like myoviruses from diverse hosts and environments. *Environ. Microbiol.* **12**, 3035–3056 (2010).
- Zeng, Q. & Chisholm, S. W. Marine viruses exploit their host's two-component regulatory system in response to resource limitation. *Curr. Biol.* **22**, 124–128 (2012).
- Wikner, J. *et al.* Nucleic acids from the host bacterium as a major source of nucleotides for three marine bacteriophages. *FEMS Microbiol. Ecol.* **12**, 237–248 (1993).
- Wilson, W. H., Carr, N. G. & Mann, N. H. The effect of phosphate status on the kinetics of cyanophage infection in the oceanic cyanobacterium *Synechococcus* sp. Wh78031. *J. Phycol.* **32**, 506–516 (1996).
- Cohen, S. S. The synthesis of nucleic acid by virus-infected bacteria. *Bacteriol. Rev.* **15**, 131–146 (1951).
- Kozloff, L. M. & Putnam, F. W. Biochemical studies of virus reproduction: III. The origin of virus phosphorus in the *Escherichia coli* T6 bacteriophage system. *J. Biol. Chem.* **182**, 229–243 (1950).
- Middelboe, M. *et al.* Virus-induced transfer of organic carbon between marine bacteria in a model community. *Aquat. Microb. Ecol.* **33**, 1–10 (2003).
- Shelford, E. J. *et al.* Virus-driven nitrogen cycling enhances phytoplankton growth. *Aquat. Microb. Ecol.* **66**, 41–46 (2012).
- Poorvin, L. *et al.* Viral release of iron and its bioavailability to marine plankton. *Limnol. Oceanogr.* **49**, 1734–1741 (2004).
- Zhao, Y. *et al.* Abundant SAR11 viruses in the ocean. *Nature* **494**, 357–360 (2013). **This paper provides the first description of viruses that infect pelagibacteria spp., which are the most abundant heterotrophic bacterium in the oceans.**
- Clasen, J. L. *et al.* Evidence that viral abundance across oceans and lakes is driven by different biological factors. *Freshw. Biol.* **53**, 1090–1100 (2008).
- Wilhelm, S. W. & Matteson, A. R. Freshwater and marine viroplankton: a brief overview of commonalities and differences. *Freshw. Biol.* **53**, 1076–1089 (2008).

37. Danovaro, R. *et al.* Marine viruses and global climate change. *FEMS Microbiol. Rev.* **35**, 993–1034 (2011).
38. Brum, J. R., Schenck, R. O. & Sullivan, M. B. Global morphological analysis of marine viruses shows minimal regional variation and dominance of non-tailed viruses. *ISME J.* **7**, 1738–1751 (2013).
This study provides quantitative estimates of the size and morphology of virus particles in seawater and provides constraints on the probable ranges of marine virus sizes.
39. Ridal, J. J. & Moore, R. M. Dissolved organic phosphorus concentrations in the northeast subtropical Pacific Ocean. *Limnol. Oceanogr.* **37**, 1067–1075 (1992).
40. Clark, L. L., Ingall, E. D. & Benner, R. Marine phosphorus is selectively remineralized. *Nature* **393**, 426–426 (1998).
41. Ammerman, J. W. *et al.* Phosphorus deficiency in the Atlantic: an emerging paradigm in oceanography. *Eos* **84**, 165–170 (2003).
42. Loh, A. N. & Bauer, J. E. Distribution, partitioning and fluxes of dissolved and particulate organic C, N and P in the eastern North Pacific and Southern Oceans. *Deep Sea Res. I* **47**, 2287–2316 (2000).
43. Lomas, M. W. *et al.* Sargasso Sea phosphorus biogeochemistry: an important role for dissolved organic phosphorus (DOP). *Biogeochemistry* **7**, 695–710 (2010).
This study shows the importance of organic, rather than inorganic, forms of phosphorus in supporting primary production in some oceanic realms (for example, in the Sargasso Sea).
44. Nausch, M. & Nausch, G. Bioavailability of dissolved organic phosphorus in the Baltic Sea. *Mar. Ecol. Prog. Ser.* **321**, 9–17 (2006).
45. Nishimura, Y., Kim, C. & Nagata, T. Vertical and seasonal variations of bacterioplankton subgroups with different nucleic acid contents: possible regulation by phosphorus. *Appl. Environ. Microbiol.* **71**, 5828–5836 (2005).
46. Raimbault, P., Garcia, N. & Cerutti, F. Distribution of inorganic and organic nutrients in the South Pacific Ocean — evidence for long-term accumulation of organic matter in nitrogen-depleted waters. *Biogeochemistry* **5**, 281–298 (2008).
47. van der Zee, C. & Chou, L. Seasonal cycling of phosphorus in the southern bight of the North Sea. *Biogeochemistry Discussions* **1**, 681–707 (2004).
48. Yoshimura, T. *et al.* Distributions of particulate and dissolved organic and inorganic phosphorus in North Pacific surface waters. *Marine Chem.* **103**, 112–121 (2007).
49. Kolowitz, L. C., Ingall, E. D. & Benner, R. Composition and cycling of marine organic phosphorus. *Limnol. Oceanogr.* **46**, 309–320 (2001).
50. Bermuda Institute of Ocean Sciences. Bermuda Atlantic Time-Series Study [online], <http://bats.bios.edu/>
51. Parsons, R. J. *et al.* Ocean time-series reveals recurring seasonal patterns of virioplankton dynamics in the northwestern Sargasso Sea. *ISME J.* **6**, 273–284 (2011).
52. Fujieki, L. A. Hawaii Ocean Time Series Data Organization and Graphical System (HOT-DOGS) [online], <http://hahana.soest.hawaii.edu/hot/hot-dogs/index.html>
53. Culley, A. I. & Welschmeyer, N. A. The abundance, distribution, and correlation of viruses, phytoplankton, and prokaryotes along a Pacific Ocean transect. *Limnol. Oceanogr.* **47**, 1508–1513 (2002).
54. Brum, J. R. Concentration, production and turnover of viruses and dissolved DNA pools at Stn ALOHA, North Pacific Subtropical Gyre. *Aquat. Microb. Ecol.* **41**, 103–113 (2005).
55. Matteson, A. R. *et al.* High abundances of cyanomyoviruses in marine ecosystems demonstrate ecological relevance. *FEMS Microbiol. Ecol.* **84**, 223–234 (2013).
56. Strzepek, R. F. *et al.* Spinning the 'ferrous wheel': the importance of the microbial community in an iron budget during the FeCycle experiment. *Global Biogeochem. Cycles* **19**, GB4S26 (2005).
57. Evans, C. & Brussaard, C. P. D. Regional variation in lytic and lysogenic viral infection in the Southern Ocean and its contribution to biogeochemical cycling. *Appl. Environ. Microbiol.* **78**, 6741–6748 (2012).
58. Evans, C., Pearce, I. & Brussaard, C. P. D. Viral-mediated lysis of microbes and carbon release in the sub-Antarctic and Polar Frontal zones of the Australian Southern Ocean. *Environ. Microbiol.* **11**, 2924–2934 (2009).
59. Hansell, D. A. *et al.* Dissolved organic matter in the ocean: new insights stimulated by a controversy. *Oceanography* **22**, 202–211 (2009).
60. Letscher, R. T. *et al.* Dissolved organic nitrogen in the global surface ocean: distribution and fate. *Global Biogeochem. Cycles* **27**, 141–153 (2013).
61. Winget, D. M. *et al.* Repeating patterns of virioplankton production within an estuarine ecosystem. *Proc. Natl Acad. Sci. USA* **108**, 11506–11511 (2011).
62. Winter, C. *et al.* Linking bacterial richness with viral abundance and prokaryotic activity. *Limnol. Oceanogr.* **50**, 968–977 (2005).
63. Matteson, A. R. *et al.* Production of viruses during a spring phytoplankton bloom in the South Pacific Ocean near of New Zealand. *FEMS Microbiol. Ecol.* **79**, 709–719 (2012).
64. Suttle, C. A., Chan, A. M. & Chen, F. *Cyanophages and Sunlight: a Paradox*. (eds Guerrero, R. & Pedros-Alio, C.) 303–307 (Spanish Society for Microbiology, 1993).
65. Bjorkman, K., Thomson-Bulldis, A. L. & Karl, D. M. Phosphorus dynamics in the North Pacific subtropical gyre. *Aquat. Microb. Ecol.* **22**, 185–198 (2000).
66. Gonzalez, J. M. & Suttle, C. A. Grazing by marine nanoflagellates on viruses and virus-sized particles: ingestion and digestion. *Marine Ecol. Prog. Ser.* **94**, 1–10 (1993).
This study shows the ecological potential for viruses to be targets of grazing.
67. Fischer, M. G. *et al.* Giant virus with a remarkable complement of genes infects marine zooplankton. *Proc. Natl Acad. Sci. USA* **107**, 19508–19513 (2010).
68. La Scola, B. *et al.* The virophage as a unique parasite of the giant mimivirus. *Nature* **455**, 100–104 (2008).
69. Steward, G. F. *et al.* Are we missing half of the viruses in the ocean? *ISME J.* **7**, 672–679 (2013).
70. Forterre, P. *et al.* Fake virus particles generated by fluorescence microscopy. *Trends Microbiol.* **21**, 1–5 (2012).
71. Dyhrman, S. T., Ammerman, J. W. & Van Mooy, B. A. S. Microbes and the marine phosphorus cycle. *Oceanography* **20**, 110–116 (2007).
72. Lindell, D. *et al.* Photosynthesis genes in marine viruses yield proteins during host infection. *Nature* **438**, 86–89 (2005).
This study shows that host-derived, viral-encoded protein expression during infection boosts host metabolism during viral progeny production.
73. Frank, H. & Moebus, K. An electron microscopic study of bacteriophages from marine waters. *Helgol. Mar. Res.* **41**, 385–414 (1987).
74. Ackermann, H.-W. & Haldal, M. in *Manual of Aquatic Viral Ecology*. (eds Wilhelm, S., Weinbauer, M. & Suttle, C.) 182–192 (American Society of Limnology and Oceanography, 2010).
75. Angly, F. E. *et al.* The marine viromes of four oceanic regions. *PLoS Biol.* **4**, 2121–2131 (2006).
76. Williamson, S. J. *et al.* The Sorcerer II Global Ocean Sampling Expedition: metagenomic characterization of viruses within aquatic microbial samples. *PLoS ONE* **3**, e1456 (2008).
77. Deng, L. *et al.* Contrasting life strategies of viruses that infect photo- and heterotrophic bacteria, as revealed by viral tagging. *mBio* **3**, e00373-12 (2012).
78. De Paeppe, M. & Taddei, F. Viruses' life history: towards a mechanistic basis of a trade-off between survival and reproduction among phages. *PLoS Biol.* **4**, e193 (2006).
79. Choi, K. H. *et al.* Insight into DNA and protein transport in double-stranded DNA viruses: the structure of bacteriophage N4. *J. Mol. Biol.* **378**, 726–736 (2008).
80. Pope, W. H. *et al.* Genome sequence, structural proteins, and capsid organization of the cyanophage Syn5: a 'horned' bacteriophage of marine *Synechococcus*. *J. Mol. Biol.* **368**, 966–981 (2007).
81. Wikoff, W. R. *et al.* Topologically linked protein rings in the bacteriophage HK97 capsid. *Science* **289**, 2129–2133 (2000).
82. Ionel, A. *et al.* Molecular rearrangements involved in the capsid shell maturation of bacteriophage T7. *J. Biol. Chem.* **286**, 234–242 (2011).
83. Tao, Y. *et al.* Assembly of a tailed bacterial virus and its genome release studied in three dimensions. *Cell* **95**, 431–437 (1998).
84. Leiman, P. G. *et al.* Structure and morphogenesis of bacteriophage T4. *Cell. Mol. Life Sci.* **60**, 2356–2370 (2003).

Acknowledgements

This work was supported by US National Science Foundation (NSF) grants OCE-1233760 (to J.S.W.) and OCE-1061352 (to A.B. and S.W.W.). This work was assisted by attendance as a short-term visitor (J.S.W.) and participation (A.B., S.W.W. and J.S.W.) in the Ocean Viral Dynamics working group at the US National Institute for Mathematical and Biological Synthesis — an Institute that is sponsored by the NSF, the US Department of Homeland Security and the US Department of Agriculture through NSF Award EF-0832858, with additional support from The University of Tennessee, Knoxville, USA. J.S.W. holds a Career Award at the Scientific Interface from the Burroughs Wellcome Fund. The authors thank participants of the Ocean Viral Dynamics working group, M. Sullivan, J. Brum and three anonymous referees for their feedback and suggestions.

Competing interests statement

The authors declare no competing interests.

DATABASES

GenBank: <http://www.ncbi.nlm.nih.gov>
NC_000866.4 | NC_008720.1 | NC_009531.1 | NC_001416.1 |
NC_002167.1 | NC_001604.1 | NC_011048

SUPPLEMENTARY INFORMATION

See online article: [S1 \(box\)](#) | [S2 \(table\)](#) | [S3 \(table\)](#) | [S4 \(table\)](#)

ALL LINKS ARE ACTIVE IN THE ONLINE PDF